



Optimization and clean synthesis of biodiesel from *Rumex crispus* leaves using calcium oxide derived from mango seed shell as a nanocatalyst

Tafere Aga Bullo¹ · Yigezu Mekonnen Bayisa¹ · Edo Begna Jiru¹ · Venkata Ramayya Ancha²

Received: 5 August 2023 / Accepted: 28 August 2023
© Akadémiai Kiadó, Budapest, Hungary 2023

Abstract

The present study investigated the synthesis of biodiesel through transesterification reaction of non-edible extracted oil from a cheap *Rumex crispus* leaves using a methanol alcohol in the presence of a nanocatalyst calcium oxide derived from mango seed shell. In line with this the synthesized calcium oxide nanocatalyst were characterized for structural patterns functional group, and energy band gap energy using XRD, FTIR and UV–Vis spectra. The effects of transesterification parameters; methanol to oil molar ratio, reaction temperature, reaction time, and catalyst loading on biodiesel yield were investigated and optimized by using a Response Surface Methodology (RSM) typically Central Composite Design (CCD). The catalyst loading turned out to be the most significant parameter with 93.72%. A 8:1 molar ratio of methanol to oil, a catalyst loading of 1.5 wt%, a reaction temperature of 65 °C and a reaction time of 3 h determines optimal conditions for the conversion of *R. crispus* leave oil to biodiesel yield of up to 93.72%. Under these conditions, the predicted and experimental biodiesel yields were 93.72% and 94.18%, respectively. The R^2 value of the model was 0.9855, indicating the accuracy of the model. The biodiesel characterization parameters met the biodiesel specifications of European Standard (EN) EN14214 and characterized by GC–MS and FTIR analysis. The biodiesel produced from *R. crispus* leaves oil as an alternative energy source could be utilized as a substitute for fossil fuels for a variety of purposes while also improving sustainable energy utilization.

Keywords Biodiesel · Transesterification · Optimization · *Rumex crispus* leave oil · Central composite design · Calcium oxide · Mango seed shell

✉ Tafere Aga Bullo
tafere.aga@ju.edu.et

¹ School of Chemical Engineering, Jimma Institute of Technology, Jimma University, P.O. Box 378, Jimma, Ethiopia

² Faculty of Mechanical Engineering, Jimma Institute of Technology, Jimma University, P.O. Box 378, Jimma, Ethiopia

Abbreviations

ANOVA	Analysis of variance
CaO	Calcium oxide
CCD	Central composite design
FTIR	Fourier transforms infrared
GC–MS	Gas chromatographs–mass spectroscopy
FAC	Fatty acids
RSM	Response surface methodology centered

Introduction

Energy is essential for improvement and central to economic improvement, destitution lessening, and continuously made strides the economy of any nation vitality utilization and demand [1]. Now a day, the problem of non-renewable energy connected with its sustainability is the major and primary issue throughout the world. In line with this, about 80% of current world energy consumption comes from non-renewable fossil fuels such as natural gas, coal and oil, the emissions of which have adverse effects on the environment and human health. During the previous decades, worldwide petroleum consumption has always increased due to the development of the human population and industrialization, which affected the depleting fossil fuel reserves and increased petroleum prices [2]. In moreover, energy demand is expected to increase due to rapid population growth, expanding urbanization, rising income levels, improved living standards, and economically feasible options to tackle the depleting fossil fuels and their harmful environmental impact [3, 4].

Currently, various analysts have conducted numerous tests ponders on biodiesel to discover options arrangement to vitality toward fuel for diesel motors without alteration, and the request of clean economic vitality sources [5, 6]. Biodiesel is the foremost promising elective diesel fuel, it has gotten a part of consideration in later a long time, as worldwide vitality request has expanded [7, 8]. A convenient way to lower the use of fossil fuels is by using biomass as a potential source of energy rather than treating them as waste.

Biomass are the most alternatives renewable energy to fossil fuels energy, used globally for 15% of the primary energy supply [9]. Consequently, biodiesel has received a lot of attention in recent years due to its advantages over nonrenewable source, since it is biodegradable, renewable, non-toxic, and emits less gaseous and particulate pollutants with higher cetane numbers than regular diesel. In addition, the growing global energy demands that are heavily dependent on oil-based fuel resources will be depleted in the near future, if current energy consumption patterns continue [10]. From a variety of agricultural waste, biodiesel fuel can be produced.

In agricultural land, *Rumex crispus* leaves is common on waste ground and a very serious weed throughout the world, because of the ability to flower numerous times annually, and production of a huge number of seeds per plant, which remain viable in the soil for many years to survive, and ability to re-grow from vegetative fragments left in the soil after cultivation or cutting [11, 12]. Thus, a cheaper feed-stock of *R. crispus* leaves oil can be used to improve the economics of biodiesel,

which will lower the price of petroleum diesel. Besides, recycles *R. crispus* leaves rather than discarded as wastes, and resolves environmental problems regarding the usage of fossil fuels. The production of fuel quality biodiesel from these different feedstock types can also be produced on a number of possible routes. Examples of such methods are homogeneous and heterogeneous base catalyzed transesterification, homogeneous and heterogeneous acid catalyzed transesterification and esterification, supercritical transesterification or enzymes catalyzed transesterification and esterification [13]. Nanocatalysts, ionic liquid catalysts and membrane technologies have been the latest [14]. Catalyst plays an important role in the production of biodiesel. In line, various heterogeneous and homogeneous catalysts have been used for the production of biodiesel. Homogeneous catalysts have drawbacks such as low FFA and moisture tolerance and complex purification processes.

On the other hand, researchers are considering heterogeneous catalysts instead of homogeneous catalysts to eliminate this cause [15]. Heterogeneous catalysts have many advantages over homogeneous catalysts such as recycling, reuse, easily separated from the product, and can be designed to give higher selectivity and longer life leads to economical production costs. However, heterogeneous catalysts also have many disadvantages such as resistance to mass transfer, time consumption, rapid deactivation, and inefficiency [16]. In moreover, metal oxide nanoparticles offer a wide range of uses in the production of green energy heterogenous catalysts. They are regarded as an active catalyst for the generation of biodiesel as green energy, as nanocatalysts are gaining popularity due to enhanced performance in terms of surface area during the transesterification reaction [17]. The current study, investigated that the capability of using mango seed shell to synthesis the calcium oxide nanoparticles a heterogenous noncatalytic for production of clean biodiesel from *R. crispus* leaves oil.

In this work, optimization and investigation of the effects of the most important independent process variables that affect the production of biodiesel (methyl ester) yield through transesterification reaction using CaO as a solid heterogeneous catalyst to attain optimal conditions by response surface methodology (RSM) via central composite design (CCD) were studied. The molar ratio of methanol to oil, reaction temperature, reaction time, and concentration of catalyst is the parameters that varied with considering the constant stirring rate. The composition of fatty acids (FAC) and the properties of biodiesel are estimated according to the standards ASTM D6751 and EN14214, and FTIR and GC-MS chromatographs are to identify the functional groups, and composition of biodiesel.

Materials and methods

Materials and reagents

The fresh *R. crispus* leaves were collected from near Jimma University and the Mango seed shell were collected from Jimma City, Jimma Ethiopia. The chemical n-hexane (99%), methanol (99.8%), and sulphuric acid (98%), were purchased from

Chem-Supply Kirkos Ltd. in Addis Ababa, Ethiopia, these used chemicals were pure analytical grade.

Methods

The collected leaves of *R. crispus* were separated manually for drying purposes and washed with distilled water several times to remove any impurities, and unwanted materials from the leave. Consequently, dried at 105 °C for 3 h in an oven until constant weight, to determine the moisture contents, and milled to a fine powder with a mortar and pestle, and kept in room temperature until extracted oil.

Extraction of *Rumex crispus* leaves oil

The prepared *R. crispus* leaves and prepared powder was used for the oil extraction by Soxhlet extractor with n-hexane as a solvent [17, 18]. The extracted crude oil was kept in a water bath at 70 °C using a rotary evaporator until the solvent n-hexane was recovered. The oil was placed in an oven at 60 °C for 15 min to remove any remaining solvent in the separated oil, and stored at 4 °C in plastic-lipped bottles, and used as a raw material for the production of biodiesel [8]. The oil yield extracted by Soxhlet extraction was estimated in percentage using Eq. 1.

$$\text{Oil Yield (\%)} = \frac{\text{Weight of extracted oil (g)}}{\text{Weight of powderd Rumex crispus leaves and roots (g)}} \cdot \quad (1)$$

Catalyst preparation

To prepare a heterogeneous catalyst from the collected waste mango seed shell were thoroughly washed two or three times with distilled water and placed in an oven at 105 °C for a day to dry completely. Then the dried mango seed shell was heated to 650 °C at a rate of 10 °C/min for 3 h to ensure the calcination process. The calcined mango seed shell was ground using a mortar and pestle [19]. The powder (CaO) was stored at room temperature. Subsequently, the prepared catalyst was refluxed and stirred in methanol for 1 h, centrifuged, and then placed in a furnace at a temperature of 650 °C (temperature rise of 5 °C/min) for 1 h. The catalyst produced was stored in a desiccator in a polyethylene container to prevent absorption of water and used for transesterification reaction to produce biodiesel with methanol in the presence of a heterogeneous catalyst (CaO).

Design of experimental and statistical analysis for optimization

Design-Expert software (version 13.0), was used to optimize the process variables and to predict the percentage yield of the response obtained at the design points and determine the optimal operating parameter for producing the maximum yield of biodiesel by the transesterification process without adversely affecting process

parameters [20]. Response surface methodology (RSM) were used in this study to examine various independent process variables for biodiesel production from *R. crispus* leaves oil utilizing a heterogeneous (CaO) catalyst based on the analysis of variance (ANOVA) has a significant impact on biodiesel yield through the transesterification process. The statistical analysis saves time, raw materials, and other costs associated with running experiments. The four independent process variables selected for this work are shown in Table 1. This range level of the factors were selected by initial tests carried out on the effects of the individual factors on the biodiesel yield and the operating limits of the production process conditions are shown in Table 1 with the coded symbols, ranges, and levels of the studied factors.

Transesterification process using a heterogeneous CaO catalyst

The transesterification reaction was carried out to produce biodiesel from oils extracted from *R. crispus* leaves, and convert oils or triglycerides (TAG) to methyl esters (biodiesel) via methanol (FAME) in the presence of a catalyst calcium oxide.

Biodiesel production from *R. crispus* leaves oil in presence of heterogeneous CaO catalyst was conducted in three-neck flasks (50 mL) under a variety of independent operating process parameters was adjusted in Table 1. The right quantity of methanol was combined with the right quantity of CaO catalyst and added to preheated the *R. crispus* leaves oil at the right temperature to carry out the transesterification reaction. To prevent the evaporation of methanol in the extract mixture, the temperature value is below the boiling point of methanol (nearly 65 °C) [21]. The transesterification reaction was carried out in all tests at a constant mixing rate of 500 rpm [22].

Upon completion of the transesterification reaction, the generated catalyst and glycerol were separated from the biodiesel by centrifuging and a funnel. The solution was transferred to a separator funnel and the mixture was allowed to settle down for 24 h to form two layers. The upper layer is biodiesel and the lower layer is glycerol [23]. Once the glycerol and FAME phases were separated, the last phase was washed with distilled water to remove any residual catalyst, glycerol, and soap [20]. The washing process was continued until the pH reached 7 (after three successive rinsing with water).

Finally, the produced biodiesel was heated in a rotary evaporator at 90 °C for 50 min to entirely separate the methanol from the biodiesel [19]. Once the biodiesel

Table 1 Selected independent process variables

Factors/variables	Symbols	Units	Range and levels	
			-1	+1
Methanol-to-oil molar ratio (v/v)	A	mL	6:1	8:1
Reaction temperature	B	°C	55	65
Reaction time	C	h	3	5
Catalyst concentration	D	wt%	0.5	1.5

has been produced, the percentage yield of biodiesel through transesterification reaction was calculated at each stage using Eq. 2.

$$\% Y = \frac{\text{Weight of methyl esters produced}}{\text{Weight of raw oil used}} \times 100. \quad (2)$$

Characterization of catalyst, *Rumex crispus* leaves oil, and its biodiesel

FT-IR analysis (PerkinElmer spectrometer) was performed to investigate the functional groups of the extracted oil, catalysts, and produced biodiesel. FT-IR analyzes were performed in the range of 500–4000 cm^{-1} . To measure the functional groups in the oil and biodiesel, droplets were poured onto the KBr plate, the second plate was placed on the first plate (sandwich mode) and the oil was converted to a thin film. To measure the functional groups of the catalyst, 1 mg of catalyst powder was first mixed with completely dried potassium bromide (KBr). After that, a small amount was poured into a special mold and pressed with a hydraulic press to obtain a transparent tablet, and finally, the FT-IR analysis was performed [24].

The physicochemical properties of extracted oil from *R. crispus* leaves oil and biodiesel was characterized by kinematic viscosity, viscosity, density, specific gravity, acid value, calorific value, saponification number, and iodine value, which were analyzed according to international standard of ASTM D 6751 and EN 14214.

Results and discussion

In this study, the relationship between the yield of biodiesel as a response and four operating conditions, methanol-to-oil molar ratio, reaction temperature, reaction time, and catalyst concentration was investigated. Thirty (30) experiments were performed based on the response surface methodology (RSM) matrix, and the results were examined (Table 3), and optimized the transesterification variables using the CCD.

Characterization of catalyst

The prepared calcined mango seed shell (MSS) were characterized by FTIR analysis to determine their functional groups of various compounds found in calcined Mango seed shell. Fig. 1 shows the results of an FT-IR analysis of the CaO sample prepared from waste mango seed shell in the range of 400–4000 cm^{-1} . Thus, observed peaks peak at 3450 cm^{-1} ; indicating that the stretching vibration associated with hydroxyl (OH) and carbonyl functional groups in the single bond region of the calcined mango seed shell, while the faint bands in 2920 cm^{-1} delivered to C–H asymmetrical stretch. Furthermore, the peaks observed in the range of 1590 and 1290 cm^{-1} were assigned to the pyrone C=C and C=O to the carboxyl group correspondingly, and the presence of C–O stretch at wavenumber 1200 cm^{-1} indicates the presence of alkoxy functional class and 1452 cm^{-1} which is a characteristic

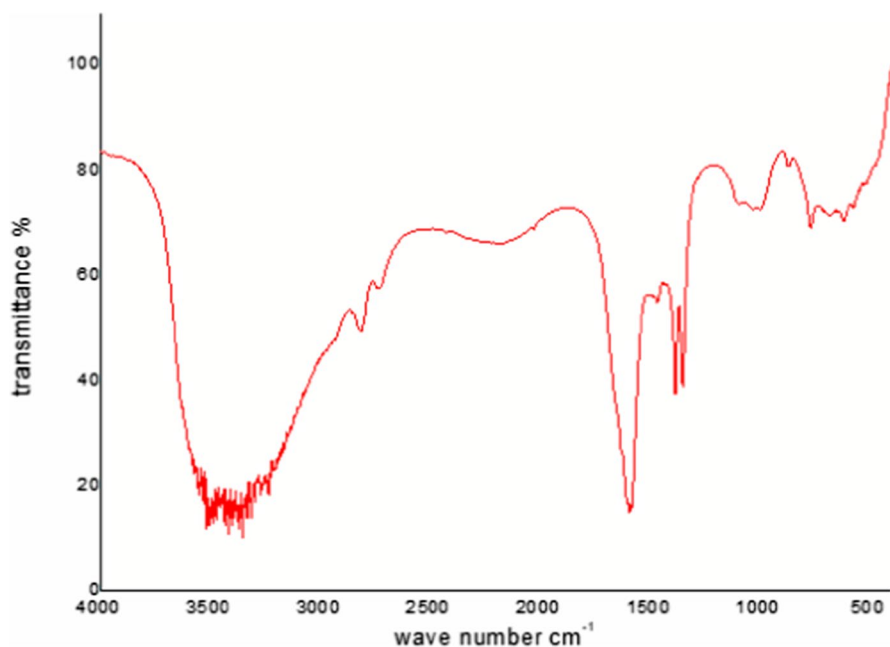


Fig. 1 Fourier transform infrared spectra of calcined mango seed shell

of C–O bond showing a bond between the oxygen atom of carbonate and calcium atom. In line with this, CaO nanoparticles depicted peaks at 1325 cm^{-1} , 1059 cm^{-1} , and 865 cm^{-1} which was attributed to the C–O bond, showing the presence of calcium oxide nanoparticle carbonation. The peak in the region of $1200\text{--}900\text{ cm}^{-1}$ is also associated with the expansion and contraction of CaO, Si–O, C–O in alcohol and ether.

The arrangement of calcium oxide (CaO) within the synthesized catalyst is identified by the XRD technique, and the comes about of this examination are appeared in Fig. 2. The results reveal that similar reflections of CaCO_3 calcite crystal phase, where characteristic peaks are observed at $2\theta = 23.2^\circ$, 29.0° , 43.0° and 47.7° , while calcium oxide formation peaks are observed at $2\theta = 32.2^\circ$, are observed in the results obtained for the mango seed shell catalyst. Calcites are presented as amorphous structures because of their synthesis from MSS biomass. The presence of calcium carbonate, which constitutes the major component in MSS, is associated with high concentrations of calcium oxide. The average crystallite size of the calcined mango seed shell nanocatalyst was calculated using the Debye–Scherrer equation (Eq. 3).

$$d = \frac{k\lambda}{\beta \cos\theta} \quad (3)$$

Here D is the crystallite size of calcined MSS in nm, K is the Scherrer shape factor (0.90), λ is the X-ray wavelength used (1.5406 \AA), β is the full width at half maximum

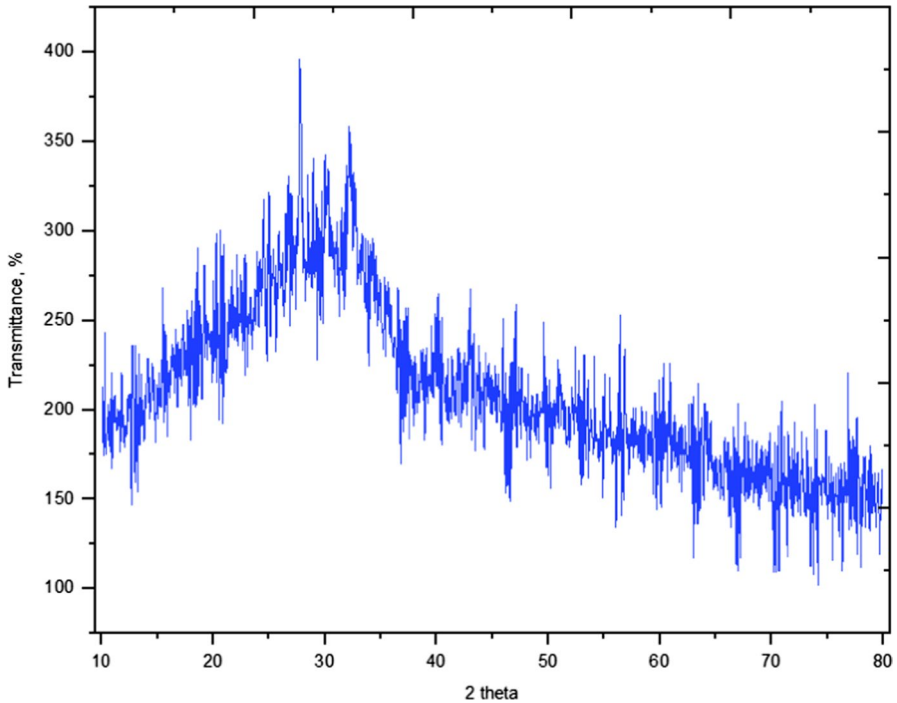


Fig. 2 X-ray diffraction (XRD) analysis of calcined mango seed shell

in radians and, θ is the Bragg diffraction angle in degrees. In this way, the normal molecule sizes of calcined MSS were anticipated as 16.4 nm. This could be happened amid the impregnation prepare of the calcined MSS.

Fig. 3 shows the ultraviolet–visible absorbance spectra in terms of absorbance of calcined mango seed shell. The shift of the absorption peak from approximately 665 nm has been shown in Fig. 3 to indicate that a sample is capable of absorbing visible light.

In accordance with the results, a reduction in the unnecessary bandgap is evident from typical optical band gap energy values of calcined mango seed shell. Therefore, the band gap has lowered from 2.2 to 1.6 eV. This result is due to a carbonate anion in the calcined mango seed shell catalyst which limits the surface area that can absorb light.

The bandgap energies of obtained calcined mango seed shell with the wavelength from UV–Vis absorption spectra were calculated using Eq. 3.

$$\text{Band gap (eV)} = \frac{1240}{\text{wavelength}}. \quad (4)$$

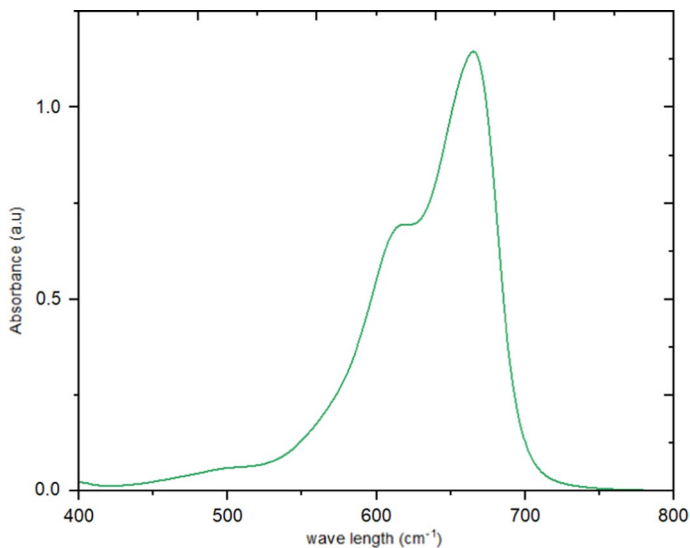


Fig. 3 Ultraviolet–visible spectra of calcined mango seed shell

Characterization of *Rumex crispus* leaves oil and produced biodiesel

The density of the oil is 900 kg/m^3 , which is consistent with the density according to ASTM D6751 and EN 14214. The acid and saponification values of the oil were determined using standard titration methods, and by using the procedure described by [25]. The density at $15 \text{ }^\circ\text{C}$ was measured with a densimeter [25, 26]. The kinematic viscosity was measured using a viscometer, and the kinematic viscosity was estimated using the density and kinematic viscosity at $40 \text{ }^\circ\text{C}$. The acid value of *R. crispus* leaves oil is 1.5 mg KOH/g , and free fatty acids are half of the acid value is 0.75.

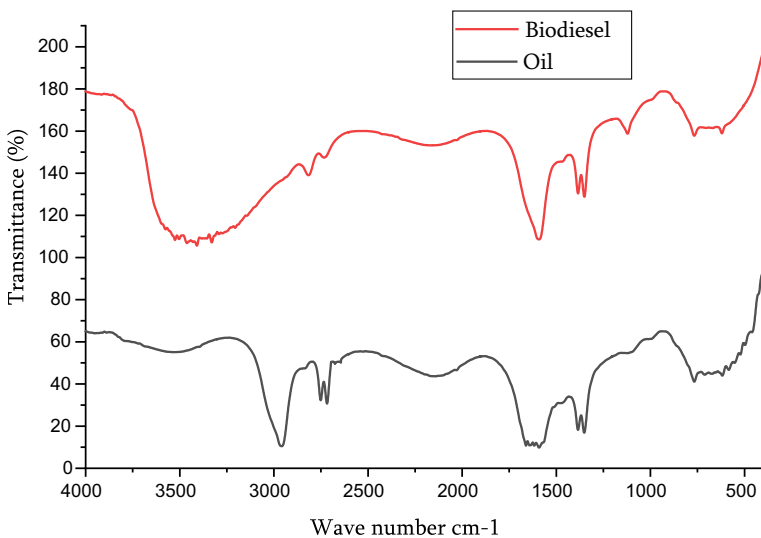
Table 2 summarizes the physicochemical properties (i.e. density, viscosity, acid value, iodine value, and saponification value) of *R. crispus* leaves oil and produced biodiesel based on the standard methods of ASTM D6751 and EN 14214. These have been significantly improved and meet the required specifications. This result shows that the *R. crispus* leaves oil can be used as substitute feedstock for the production of biodiesel.

FT-IR analysis of *Rumex crispus* leaves oil and biodiesel

The infrared spectrum (FT-IR) analysis of the Fourier transforms of produced biodiesel shown in Fig. 4 was used for quantitative analysis. The peak in the spectrum represented the functional groups contained in the oil. The wave number, functional group, band assignment, and absorption intensity of the absorption peaks were detected in the infrared spectrum of the Fourier transform of oil, and biodiesel. Fig. 4 shows the FTIR spectrum of the extracted oil and biodiesel in the range of 400 to 4000 cm^{-1} . The broad bond in the range of 1813 – 2678 cm^{-1} was attributed

Table 2 Summarized the physico-chemical of the *Rumex crispus* leaves oil, and produced biodiesel in United States standards (ASTM D-67510 and Europe (EN 14214)

Property	Units	<i>Rumex crispus</i> leaves oil	Biodiesel Yields	EN 14214	ASTM D-6751	References
pH	–	6.65	7.85	5–6.7	7–9	[7, 8, 25–28]
Density at 15 °C	kg/m ³	900	895	860–900		
Specific gravity	–	0.90	0.895	0.86–0.9		
Kinematic viscosity at 40 °C	CSt	3.88	4.6	3.5–5.0	1.9–6.0	
Flashpoint	°C		132.5	> 120	> 130	
Calorific value	MJ/kg	37.5	38.57			
Yield	%	35.8	94.45			
Cetane number		55	50.5	> 51	> 47	
Iodine value	mg I ₂ /100 g	92.5	109.45	< 120		
Acid value	mg NaOH/g	1.55	0.325		< 0.5	
Free fatty acids		0.775	0.1625			
Saponification value	mg KOH/g	186.5				

**Fig. 4** FT-IR spectra of extracted oil, and biodiesel

to the stretching mode of the O–H groups, as well as weak bond of the OH– bending vibration at 1600 cm^{-1} , which occurred due the adsorption of water molecules from the air on the surface of the catalyst. The carbon–hydrogen bonds formed at $625\text{--}3330\text{ cm}^{-1}$, the functionality of the ester at $1715\text{--}1750\text{ cm}^{-1}$, the terminal carbons CH_3 at $1354\text{--}1589\text{ cm}^{-1}$, and the carbon–oxygen bonds at $762\text{--}1120\text{ cm}^{-1}$. The results demonstrate that the produced biodiesel is composed of long-chain fatty acid esters. The transesterification process are chemically similar to the refined oil, the CaO stretch peak is 1663 cm^{-1} located in the range $2966\text{--}611\text{ cm}^{-1}$ is typical of esters, the spectrum is often found in FAME and refined oil.

GC–MS analysis of biodiesel

GC–MS (gas chromatography–mass spectrometry) was performed to determine the composition of the methyl ester. While using GC–MS, we should always consider two important pieces of information: retention time (RT) and peak area (PA). However, due to the unique physical properties of the sample, the RT must remain constant as long as the analytical method is the same. It is also important to understand the elution order of the compounds in the mixture before the GC–MS analysis of the sample. Fig. 5, shows the chromatogram of biodiesel with the presence of derivatives of (a) $\text{C}_{16:0}$ (palmitic acid methyl ester), (b) $\text{C}_{17:0}$ (methyl heptadecanoate), (c) $\text{C}_{18:1}$ (oleic acid methyl ester), (d) $\text{C}_{18:2}$ (linoleic acid methyl ester), (e) $\text{C}_{18:3}$ (linolenic acid methyl ester), (f) diglycerides, (g) unreacted triglycerides present in the biodiesel. The chromatogram of biodiesel obtained from *R. crispus* leaves oil confirmed the formation of methyl esters.

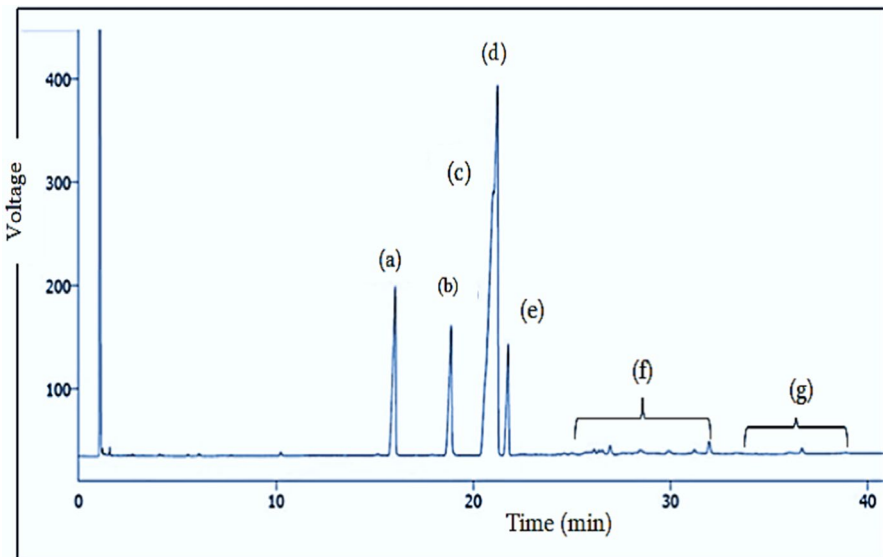


Fig. 5 GC–MS chromatogram of biodiesel

Optimization of operating variables by statistical analysis via response-surface methodology (RSM)

The quadratic regression model is used to investigate the effects of numerous independent operating variables on the produced biodiesel. The commonly statistical schemes used for response surface methodology (RSM) are central composite designs (CCD), which can be used under certain parametric conditions. RSM was used to optimize the interaction of four variables: the methanol to oil ratio, reaction temperature, reaction time, and catalyst loading. Analysis of variance (ANOVA) based on the analysis of parameters that have a significant impact on biodiesel yield through the transesterification process from *R. crispus* leaves oil biodiesel yields ranged from 74.14 to 94.18%. Table 3 shows the results of the central composite design (CCD) model for optimizing the process parameters. These results indicate that biodiesel yields vary by the production process. All running orders have been randomized to avoid systematic errors.

The predicted biodiesel yield values were generated from a quadratic regression model taken from the statistical analysis of experimental data using response surface methodology (RSM). The response surface methodology was used to calculate the effect of each parameter and its interaction with other parameters. The response (biodiesel yield %) was correlated with other parameters using a full quadratic regression model shown in Eq. (3). This model represents the predicted yield (Y) of *R. crispus* leaves oil biodiesel as a function of methanol:oil molar ratio (A), reaction temperature (B), reaction time (C), and catalyst concentration (wt%) (D).

$$\begin{aligned}
 Y = & 84.62 + 0.5498A - 0.6391B - 0.7479C \\
 & - 0.3333D + 1.67AB + 0.5863AC + 2.96AD \\
 & - 0.2925BC + 0.7525BD - 3.56CD - 0.0827A^2 \\
 & - 0.0174B^2 + 0.2136C^2 + 0.0026D^2.
 \end{aligned} \tag{5}$$

This model equation in terms of coded factors shows that the positive coefficients are A, AB, AC, AD, BD, A², C², and D², which are the high levels of the factors and the negative coefficients are B, C, D, A², B² and the interaction of BC, and CD are the low levels of the factors. The final coded equation is useful for identifying the relative impact of factors by comparing the coefficients of the factors. The estimated coefficient represents the expected response changes per unit change in the factor by assuming that all remaining factors are constant. Table 4 shows the importance of these parameters related to the probability value (p-value).

Analysis of variance (ANOVA) is performed to determine the significance and validity of the quadratic model, as well as the effects of individual significant terms and interactions on the selected responses [29]. As the ANOVA results are shown in Table 4, the quadratic regression model has an F-value (73.01) higher and implies the model is significant and a p-value or probability error value is used to check the significance of each regression coefficient which is (0.0001) lower than the significance level ($p < 0.05$), indicating that the model terms are significant. In this case, A, B, C, D, AB, AC, AD, BD, and CD are significant model terms, and values

Table 3 Experimental central composite design result for the optimization of parameters of the transesterification process for the biodiesel yield (%) from *Rumex crispus* leaves oil

Exp. no.	Run order	A: methanol to oil molar ratio	B: temperature (°C)	C: reaction time (h)	D: CaO (wt%)	<i>Rumex crispus</i> leaves oil biodiesel yield (%)	
						Experimental/actual value	Predicted value
1	9	6	55	3	1.5	87.2	87.05
2	20	7	67.07	4	1	83.5	83.68
3	19	7	52.93	4	1	85.75	85.49
4	13	6	55	5	1.5	78.28	77.84
5	15	6	65	5	1.5	74.14	74.14
6	5	6	55	5	0.5	92.45	93.07
7	4	8	65	3	0.5	79.5	79.82
8	17	5.586	60	4	1	83.98	83.68
9	21	7	60	2.58579	1	87.01	86.10
10	26	7	60	4	1	84.62	84.62
11	29	7	60	4	1	84.63	84.62
12	3	6	65	3	0.5	82.42	82.48
13	14	8	55	5	1.5	82.6	82.70
14	30	7	60	4	1	84.65	84.62
15	11	6	65	3	1.5	83.95	84.52
16	23	7	60	4	0.29289	85.48	85.10
17	24	7	60	4	1.70711	83.85	84.15
18	22	7	60	5.41421	1	83.1641	83.99
19	10	8	55	3	1.5	89.12	89.56
20	8	8	65	5	0.5	85.74	86.04
21	6	8	55	5	0.5	86.76	86.07
22	12	8	65	3	1.5	94.18	93.72
23	18	8.41421	60	4	1	85.0089	85.23
24	7	6	65	5	0.5	86.92	86.36
25	27	7	60	4	1	83.6112	84.62
26	25	7	60	4	1	84.62	84.62
27	28	7	60	4	1	85.42	84.62
28	16	8	65	5	1.5	86.15	85.68
29	1	6	55	3	0.5	87.67	88.02
30	2	8	55	3	0.5	78.52	78.68

greater than 0.1000 indicate that the model terms are not significant. If there are many insignificant models, this implies reduction may improve the model.

The lack of fit is also determined by the quadratic regression model, which shows a lack of fit, this indicates that the model does not sufficiently describe the relationship between the independent variables (i.e. the methanol to oil molar ratio, the reaction temperature, the reaction time and the concentration of the

Table 4 Results obtained from analysis of variance (ANOVA) for the quadratic model

Factors	Sum of squares	Df	Mean square	F-value	p-value (Prob > F)	Remarks
Model	432.59	14	30.90	73.01	<0.0001	Significant
A-molar ratio of methanol to oil	6.04	1	6.04	14.28	0.0018	
B-reaction temperature	8.17	1	8.17	19.30	0.0005	
C-reaction time	11.19	1	11.19	26.44	0.0001	
D-catalyst concentration	2.22	1	2.22	5.25	0.0369	
AB	44.69	1	44.69	105.59	<0.0001	
AC	5.50	1	5.50	12.99	0.0026	
AD	140.54	1	140.54	332.08	<0.0001	
BC	1.37	1	1.37	3.23	0.0923	
BD	9.06	1	9.06	21.41	0.0003	
CD	203.35	1	203.35	480.48	<0.0001	
A ²	0.0638	1	0.0638	0.1507	0.7033	
B ²	0.0028	1	0.0028	0.0067	0.9360	
C ²	0.4259	1	0.4259	1.01	0.3317	
D ²	0.0001	1	0.0001	0.0001	0.9904	
Residual	6.35	15	0.4232			Not significant
Lack of fit	4.69	10	0.4694	1.42	0.3670	
Pure error	1.65	5	0.3308			
Cor total	438.94	29				
R ²	0.9855		Adjusted R ²	0.9720		
Mean	84.70		Predicted R ²	0.9303		
CV % ^a	0.7681		Adeq precision	42.5651		

^aCoefficient of variation

catalyst) and the dependent variable (i.e. biodiesel yield). In this study, the F and p-value of the fit parameter were found to be 1.42 and 0.3670, respectively. The p-value of the missing adjustment parameter is greater than 0.0500, indicating that there is a good fit between the quadratic regression model and the experimental data.

The coefficient of determination R-squared (R^2) reflects the variability of the dependent variable explained by its relationship with the independent variables (predictive variables). In general, a high R^2 value indicates that the model is responsible for more data variability and therefore the data points will be closer to the regression line. In other words, a high R^2 value indicates a good fit between the model and the experimental data. Based on the results of Table 4, it can be seen that the R^2 value is 0.9955, indicating that 99.55% of the variability of biodiesel yield is explained by the quadratic regression model.

However, it should be noted that the value of R^2 can increase as the number of predictive variables in the model increases and therefore care must be taken in interpreting the value. The corrected coefficient of determination (adjusted R^2) is used to compensate for this undesirable effect, as it not only indicates how well the model fits the experimental data but also takes into account the number of predictive variables. Adjusted R^2 will increase if useful predictive variables are added to the model, and likewise, adjusted R^2 will decrease as unnecessary predictor variables are added. The adjusted R^2 is 0.9720 as shown in Table 4, indicating that the model accounts for 97.20% of the variation in biodiesel yield.

The predicted and experimental values of the biodiesel yield are shown in Fig. 6, as the line of a perfect fit with the point corresponding to the zero error. The differences between the experimental and predicted values appear to be less than 0.2, indicating good agreement between the model and the experimental data. A point close to a straight line indicates that the experimental and predicted values are in good agreement. This result is consistent with R^2 obtained earlier and R^2 modified to a value close to unity. Therefore, the regression model gives a good estimate of system response (i.e. biodiesel yield) with changes in process variables.

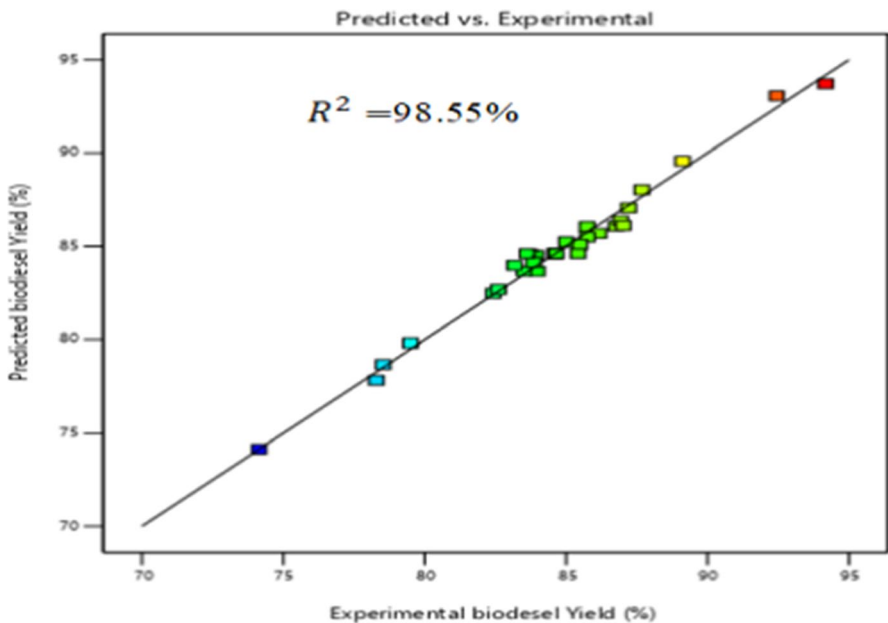


Fig. 6 Plots of the experimental versus predicted biodiesel yield (%)

Effect of process variables on biodiesel yield

This study examines the effect of the molar ratio of methanol to oil on the biodiesel yield by varying the methanol to oil ratios within the ranges of 6 : 1 – 8 : 1. The most effective variable affecting the conversion efficiency of the produced methyl ester yield during the transesterification reaction is the molar ratio of alcohol (methanol) to extracted oil. Since transesterification is an equilibrium reaction, a large excess of alcohol is required for the reaction to proceed and avoid the reversible reaction [30].

Fig. 7a shows the three-dimensional surface plot of the combined effects of methanol to oil molar ratio and catalyst concentration on biodiesel yield. Finding the appropriate methanol-to-oil ratio is critical in determining the methyl ester yield. If the methanol to oil ratio is insufficient for the transesterification reaction, glycerides will not be converted to fatty acid methyl esters, resulting in lower biodiesel yields. In general, it can be observed that at a fixed catalyst concentration increasing

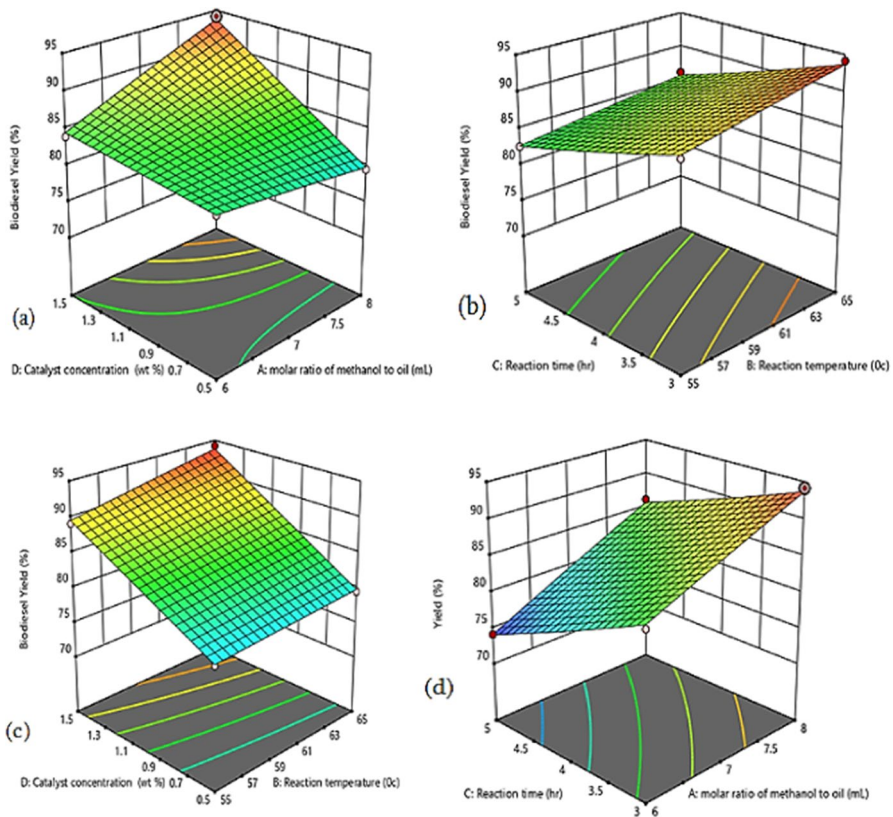


Fig. 7 Three-dimensional contour plot, which shows the combined effects of **a** catalyst concentration and molar ratio methanol to oil, **b** reaction time and reaction temperature, **c** catalyst concentration and reaction temperature, and **d** reaction time and molar ratio methanol to oil on the biodiesel yield

the methanol to oil molar ratio has an insignificant effect on the yield of biodiesel. Increasing the amount of methanol increases the time required to extract excess methanol from biodiesel after the transesterification process since methanol has a polar hydroxyl group that acts as an emulsifier and thus improving the solubility of glycerol in the biodiesel phase and ultimately lowering the yield. In general, adding excessive amounts of methanol to oil are not recommended, because it decreases the percent methyl ester yield, this behavior indicates that the separation of glycerol and methyl esters becomes more difficult due to the emulsification and reversibility behavior of the transesterification reaction [24]. The maximum biodiesel yield was achieved at methanol to oil molar ratio of 8:1, keeping the catalytic concentration and reaction temperature at their optimal values. This fact indicates that excess alcohol in the transesterification process will tip to rises in the product, while the opposite side of excess methanol increases glycerol solubility, resulting in lower yields.

Fig. 7b shows the effect of reaction temperature and reaction time on biodiesel yield when the molar ratio of methanol to oil and catalyst load are held constant at 8:1 and 1.5 wt%. Fig. 7b shows that the maximum biodiesel yield could be achieved with a reaction time of 3 h. A further increase in the reaction time will not affect the biodiesel yield. This could be recognized in the reverse reaction loading to reduce FAME formation. The optimal value of the reaction temperature is observed at 65 °C.

The reaction temperature has a significant influence on the reaction rate and the conversion to methyl ester. The biodiesel yield increases with increasing reaction temperature, but approached the boiling point of methanol, the biodiesel yield decreases. Concerning the reaction time, the effect of the reaction temperature influences the yield to the maximum. However, compared to reaction time, the effect of reaction temperature has the greatest impact on yield [31].

Fig. 7c, shows the three-dimensional surface plot of the combined effects of temperature and catalyst concentration on FFA conversion with other variables (i.e., methanol to oil molar ratio and reaction time) kept constant at their mean values (8:1 and 3 h) with constant stirring speed. In fact from Fig. 7c, it can be observed that increasing the catalyst concentration from the range of 0.50 to 1.5 wt% decreases the biodiesel yield [32]. This indicates that the optimal operating parameters for the transesterification parameters of methanol to oil ratio at 8:1, reaction time at 3 h, catalyst concentration of 1.5 wt%, and reaction temperature of 65 °C with maximum biodiesel yield of 94.18%.

Fig. 7d, shows the three-dimensional surface plot of the combined effects of methanol concentration, and reaction time on biodiesel yield conversion, with other variables (i.e. reaction temperature and catalyst concentration) kept constant at their mean values (8:1 and 3 h). The contour diagram indicated that there were two optimal ranges of the methanol to oil ratio, one in the lower half of the contour diagrams and the other in the upper half of the contour diagrams [19]. In the lower half of the contour diagram, at a low ratio of methanol to oil, there was a moderate decrease in biodiesel yield with an increase in reaction time due to the negative time effect of Eq. 3.

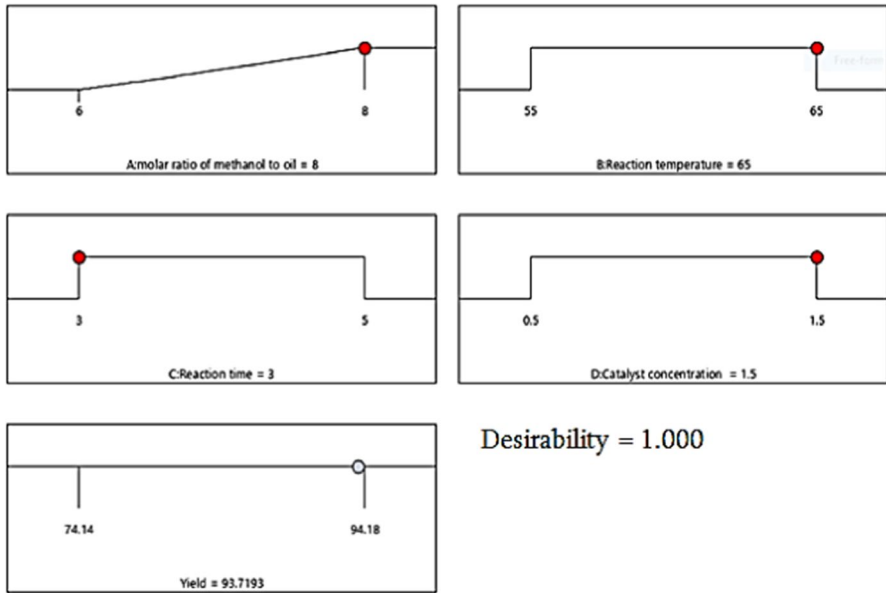


Fig. 8 Ramp graph for maximum yield with desirability 1

From Fig. 8, the ramp diagram, it can be seen that the optimum ester yield is 94.18% when the molar ratio of methanol to oil, catalyst concentration, reaction temperature, and reaction time are 8:1, 1.5 wt%, 65 °C, and 3 h.

Conclusion

This study focused on optimizing and characterizing the biodiesel production process independent parameters for biodiesel derived from non-edible feedstocks (*R. crispus* leaves oil) via transesterification reaction using response surface methodology. The response surface methodology based on the central composite design was applied to investigate the interactive effects of process parameters on the ester yield, to obtain the optimum yield of biodiesel. The optimal operating parameters for transesterification of oil at a molar ratio of methanol to oil of 8:1, a reaction temperature of 65 °C, a reaction time of 3 h, and a catalyst concentration of 1.5 wt%. These optimal operating parameters were validated with the actual biodiesel yield of 94.18%, and the predicted ester yields were 93.72% under optimized conditions. The coefficient of variance (CV %) was 0.7681 with a 98.55% confidence limit of R^2 . The physicochemical properties of biodiesel are produced to meet the requirements of ASTM D6751 and EN14214 standards. The values are close to the physicochemical properties of diesel leading to the conclusion that optimized biodiesel are a potential replacement for diesel fuel. The

results indicated that *R. crispus* leaves oil could be a possible feedstock for biodiesel production, although more studies are needed to produce a quality fuel and to evaluate the engine performance and emissions of this biodiesel.

Acknowledgements We would like to acknowledge the FT-IR Platform at the Faculty of Material Science and Engineering Faculty of Mechanical Engineering, School of Chemical Engineering Laboratory staff members at Jimma Institute of Technology for their knowledge sharing and technical support. This work was financially supported by the Jimma Institute of Technology Center of Excellence-CRGE RESOURCE CART (Climate Resilient Green Economy Resource Centre for Advanced Research and Training-Linking Energy with Water and Agriculture).

Author contributions All the authors: TA wrote the main parts of the manuscript, YM, EB and VR have made a substantial contribution in conceptualization, data curation, formal analysis, methodology, designed the study and procedure, interpretation of the data, conducting lab testing, visualization, validation, analysis of FT-IR spectroscopy, and GC-MS analysis. All authors read and approved the final manuscript.

Funding Not applicable.

Data availability The availability of data, i.e., experimental design, data analysis (RSM), FTIR, Gas chromatography-mass spectrometry (GC-MS) used to support the results of this study are incorporated in the article.

Declarations

Conflict of interest The authors declare no competing interests.

Ethical approval This article does not include human or animal studies conducted by any of the authors.

Informed consent Consent to participate in the study was also obtained at the individual level.

References

1. Palani Y, Devarajan C, Manickam D, Thanikodi S (2022) Performance and emission characteristics of biodiesel-blend in diesel engine. A review. *Environ Eng Res* 27(1):200338
2. Ahmia AC, Danane F, Bessah R, Boumesbah I (2014) Raw material for biodiesel production. Valorization of used edible oil. *J Renew Energies* 17(2):335–343
3. Bayisa YM, Bullo TA, Hundie KB (2022) Optimizing process parameter for biodiesel production from avocado peel oil using chicken eggshell biocatalysts using central composite design (CCD). *Reac Kinet Mech Cat* 135(6):3185–3203
4. Zulqarnain, Mohd Yusoff MH, Ayoub M, Ramzan N, Nazir MH, Zahid I, Butt TA (2021) Overview of feedstocks for sustainable biodiesel production and implementation of the biodiesel program in Pakistan. *ACS Omega* 6(29):19099–19114
5. Adeniyi AG, Ighalo JO, Adeoye AS, Onifa DV (2019) Modelling and optimisation of biodiesel production from *Euphorbia lathyris* using ASPEN Hysys. *SN Appl Sci* 1(11):1452
6. Olagunju OA, Musonge P, Kiambi SL (2022) Production and optimization of biodiesel in a membrane reactor using a solid base catalyst. *Membranes* 12(7):674
7. Dharma S, Hassan MH, Ong HC, Sebayang AH, Silitonga AS, Kusumo F (2017) Optimization of biodiesel production from mixed *Jatropha curcas*–*Ceiba pentandra* using artificial neural network-genetic algorithm: evaluation of reaction kinetic models. *Chem Eng Trans* 56:547–552
8. Anwar M, Rasul M, Ashwath N, Rahman M (2018) Optimisation of second-generation biodiesel production from Australian native stone fruit oil using response surface method. *Energies* 11:2566

9. Ahmia AC, Danane F, Bessah R, Boumesbah I (2014) Raw material for biodiesel production Valorization of used edible oil. *J Renew Energies* 17(2):335–343
10. Fan X, Wang X, Chen F (2011) Biodiesel production from crude cottonseed oil: an optimization process using response surface methodology. *Open Fuels Energy Sci J* 4(1):1–8
11. Iqbal MF, Shad GM, Feng YL, Liu MC, Wang S, Lu XR, Tariq M (2019) Efficacy of postemergence herbicides for controlling curled dock (*Rumex crispus* L.) in wheat crops. *Appl Ecol Environ Res* 17(6):12753–12767
12. Amini R, Bahmani Y, Amjadi E, Nazari Z (2015) Effect of salinity and crop residue on seed germination and early seedling growth of curled dock (*Rumex crispus* L.). *Int J Plant Anim Environ Sci* 5(1):68–73
13. Bullo TA, Bayisa YM, Bultum MS (2022) Biosynthesis of sulfonated carbon catalyst from carbohydrate polymer derivatives for epoxidation of *Croton macrostachyus* seed oil. *Carbohydr Polym Technol Appl* 3:100221
14. Bullo TA, Bayisa YM, Bultum MS (2022) Optimization and biosynthesis of calcined chicken eggshell doped titanium dioxide photocatalyst based nanoparticles for wastewater treatment. *SN Appl Sci* 4(1):17
15. Talebian-Kiakalaieh A, Amin NA, Mazaheri H (2013) A review on novel processes of biodiesel production from waste cooking oil. *Appl Energy* 104:683–710
16. Gupta J, Agarwal M, Dalai AK (2016) Optimization of biodiesel production from mixture of edible and nonedible vegetable oils. *Biocatal Agric Biotechnol* 8:112–120
17. Habte L, Shiferaw N, Mulatu D, Thenepalli T, Chilakala R, Ahn JW (2019) Synthesis of nanocalcium oxide from waste eggshell by sol–gel method. *Sustainability* 11(11):3196
18. Panichikkal AF, Prakasan P, Kizhakkepowathial Nair U, Kulangara Valappil M (2018) Optimization of parameters for the production of biodiesel from rubber seed oil using onsite lipase by response surface methodology. *Biotech* 8:1–14
19. El-Gendy NS, Deriase SF, Hamdy A, Abdallah RI (2015) Statistical optimization of biodiesel production from sunflower waste cooking oil using basic heterogeneous biocatalyst prepared from eggshells. *Egypt J Pet* 24(1):37–48
20. Foroutan R, Mohammadi R, Ramavandi B (2021) Waste glass catalyst for biodiesel production from waste chicken fat: optimization by RSM and ANNs and toxicity assessment. *Fuel* 291:120–151
21. Rajesh K, Devan PK, Bharth Sai Kumar GK (2021) Parametric optimization and biodiesel production from coconut fatty acid distillate. *Iran J Chem Chem Eng* 40(1):343–355
22. El Boulifi N, Bouaid A, Martinez M, Aracil J (2010) Process optimization for biodiesel production from corn oil and its oxidative stability. *Int J Chem Eng*. <https://doi.org/10.1155/2010/518070>
23. Foroutan R, Mohammadi R, Esmaili H, Bektashi FM, Tamjidi S (2020) Transesterification of waste edible oils to biodiesel using calcium oxide@ magnesium oxide nanocatalyst. *Waste Manag* 105:373–383
24. Lakshmana Naik R, Radhika N, Sravani K, Hareesha A, Mohanakumari B, Bhavanasindhu K (2015) Optimized parameters for production of biodiesel from fried oil. *Int Adv Res J Sci Eng Technol* 2(6):62–65
25. Hundie KB, Shumi LD, Bullo TA (2022) Investigation of biodiesel production parameters by transesterification of watermelon waste oil using definitive screening design and produced biodiesel characterization. *S Afr J Chem Eng* 41:140–149
26. Bullo TA, Fana FB (2021) Production and characterization of biodiesel from avocado peel oils using experimental analysis (ANOVA). *J Eng Adv* 2(02):104–111
27. Aworanti OA, Agarry SE, Ajani AO (2013) Statistical optimization of process variables for biodiesel production from waste cooking oil using heterogeneous base catalyst. *Br Biotechnol J* 3(2):116–132
28. Singh D, Kumar V, Sandhu SS, Sarma AK (2016) Process optimization for biodiesel production from indigenous non-edible *Prunus armeniaca* oil. *Adv Energy Res* 4(3):189
29. Bai L, Tajikfar A, Tamjidi S, Foroutan R, Esmaili H (2021) Synthesis of MnFe₂O₄@ graphene oxide catalyst for biodiesel production from waste edible oil. *Renew Energy* 170:426–437
30. Dharma SM, Masjuki HH, Ong HC, Sebayang AH, Silitonga AS, Kusumo F, Mahlia TM (2016) Optimization of biodiesel production process for mixed *Jatropha curcas*–*Ceiba pentandra* biodiesel using response surface methodology. *Energy Convers Manag* 115:178–190
31. Elkady MF, Zaatout A, Balbaa O (2015) Production of biodiesel from waste vegetable oil via KM micromixer. *J Chem* 2015:630168

32. Jeyakumar N, Narayanasamy B, Venkatraman B (2021) Optimisation of biodiesel production from jack fruit seed oil using response surface methodology. *Int J Ambient Energy* 42(16):1864–1875

Publisher's Note Springer Nature remains neutral with regard to jurisdictional claims in published maps and institutional affiliations.

Springer Nature or its licensor (e.g. a society or other partner) holds exclusive rights to this article under a publishing agreement with the author(s) or other rightsholder(s); author self-archiving of the accepted manuscript version of this article is solely governed by the terms of such publishing agreement and applicable law.